

# Potential of Neutrino Telescopes to Detect Quantum Gravity-Induced Decoherence in the Presence of Dark Fermions

Alba Domi<sup>\*1</sup>, Thomas Eberl<sup>†1</sup>, Dominik Hellmann<sup>‡2</sup>, Sara Krieg<sup>§2</sup>, and Heinrich Päs<sup>¶2</sup>

<sup>1</sup>Erlangen Centre for Astroparticle Physics, Friedrich-Alexander-Universität  
Erlangen-Nürnberg, Nikolaus-Fiebiger-Str. 2, 91058 Erlangen, Germany

<sup>2</sup>Fakultät für Physik, Technische Universität Dortmund, Otto-Hahn-Straße 4, 44227  
Dortmund, Germany

January 23, 2025

## Abstract

We assess the potential of neutrino telescopes to discover quantum-gravity-induced decoherence effects modeled in the open-quantum system framework and with arbitrary numbers of active and dark fermion generations, such as particle dark matter or sterile neutrinos. The expected damping of neutrino flavor oscillation probabilities as a function of energy and propagation length thus encodes information about quantum gravity effects and the fermion generation multiplicity in the dark sector. We employ a public Monte-Carlo dataset provided by the IceCube Collaboration to model the detector response and estimate the sensitivity of IceCube to oscillation effects in atmospheric neutrinos induced by the presented model. Our findings confirm the potential of very-large-volume neutrino telescopes to test this class of models and indicate higher sensitivities for increasing numbers of dark fermions.

## 1 Introduction

The most fundamental theories in physics, General Relativity (GR) and the Standard Model (SM) of particle physics, have been tested with very high precision. However, unifying these theories into a universal theory of Quantum Gravity (QG) remains one of the greatest challenges in fundamental physics [1]. Approaches like string theory or loop quantum gravity seek to integrate these theories into a more comprehensive framework, in which GR and Quantum Theory emerge as limiting cases, c.f. for example Ref.s [2–4] and [5–10]. However, to date, no experimental evidence exists favoring any of these approaches to QG, underscoring the profound difficulties all these approaches encounter [11]. Another possible avenue to study and find evidence for QG is to pursue the bottom-up approach by formulating a low energy effective theory of how QG could impact another, known quantum system. One way to formulate such an effective theory is by utilizing the open quantum system framework in which we consider the equations of motion of a known quantum system and treat QG as an environment. As extensively explored in the literature [12–25], QG effects could induce decoherence, i.e. the loss of coherence in a quantum system due to its interaction and entanglement with an environment, that is a or even the defining characteristic of the quantum-to-classical transition [26], potentially leading to

---

\*alba.domi@fau.de

†thomas.eberl@fau.de

‡dominik.hellmann@tu-dortmund.de

§sara.krieg@tu-dortmund.de

¶heinrich.paes@tu-dortmund.de

observable phenomena. It follows that the exploration of quantum gravitational effects and the quantum-to-classical transition represents an exciting research frontier.

Applying this framework to the study of neutrino flavor oscillations, QG induced decoherence could provide a useful tool in the search for unknown electrically neutral particles [27, 28], i.e. possible dark matter (DM) candidates. This conjecture is based on the central assumption that QG interactions maximally violate global quantum numbers—such as lepton flavor—while conserving only unbroken gauge quantum numbers, as discussed for example in Ref.s [29–31]. This assumption is rooted in the so called No-Hair theorem [32, 33]: Black holes only conserve energy, angular momentum and gauge charges, all other information of particles falling inside is lost. If quantum black holes in the spacetime foam share this property, this implies that flavor information of a quantum system reduces while it interacts with this environment. Furthermore, assuming the existence of new fermionic particle species being singlets with respect to the unbroken SM gauge group  $SU(3)_c \times U(1)_{em}$ , this could induce transitions between neutrinos and these unknown fermion species that are otherwise forbidden or highly suppressed. Candidates for such dark fermions include WIMPS [34], sterile neutrinos [35], and FIMPS [36]. Given that numerous searches for DM candidates have not yet produced significant evidence, it is possible that if such new particles exist, they are entirely decoupled from the Standard Model in the current phase of the universe and hence interact purely gravitationally with known matter. Therefore, besides providing a potential window on QG, the proposed mechanism offers a rare and valuable opportunity to search for these highly elusive particles.

A further consequence of the maximally flavor violating properties of QG is that information distinguishing particles of different flavor would degrade over time, resulting in fully democratic transition probabilities [27] across all generations of active neutrinos as well as the hypothetical dark fermions. Hence, an initially pure neutrino system would always develop a dark component after travelling a sufficiently long distance. This, in turn, results in distinct oscillation signatures in neutrino oscillation experiments, reflecting the influence of the dark fermions. Consequently, long baseline neutrino experiments could be sensitive to such an effect, allowing to probe the QG parameters [37–42]. Neutrino telescopes such as IceCube [43], ANTARES [44] and KM3NeT [45] have a significant advantage over the other neutrino experiments, as they can exploit a wider range of  $L/E$  ratios, allowing for high sensitivity to a broader region of the QG parameter space. Currently, no evidence for QG-induced quantum decoherence has been observed [38–41], and the most stringent limits on decoherence parameters growing with increasing energy have been established by the IceCube collaboration using high energy atmospheric neutrinos [41].

Meanwhile, the KM3NeT infrastructure is under construction in the Mediterranean Sea and features two detectors, ORCA and ARCA, each designed for studying neutrinos at different energy ranges. ORCA is optimized for detecting neutrinos with energies starting from 1 GeV, where matter effects in the Earth enhance its sensitivity to high-precision measurements of neutrino oscillations using atmospheric neutrinos. This feature allows ORCA to probe decoherence parameters decreasing with growing neutrino energy with high sensitivity. On the other hand, ARCA is designed for high-energy neutrino studies, extending to PeV energies and beyond, and offers complementary sky coverage to IceCube. Together, these experiments provide a comprehensive probe of neutrino behavior across a wide range of energy scales.

In this work, the IceCube Neutrino Observatory is of particular interest due to its extensive public dataset release, which allows to investigate the detector’s potential for testing the proposed model. We perform a statistical analysis on a pseudo data set generated according to the standard three neutrino oscillation hypothesis to investigate the potential constraints that IceCube could impose on QG parameters using atmospheric neutrinos, considering different total numbers of dark fermions and various decoherence models. Our work extends the previous IceCube analysis on quantum decoherence (QD) [41] by including a varying number of dark fermions, allowing for a generalization; when the number of dark fermions is set to zero, our results align with those of IceCube. Furthermore, the assumption that QG is maximally flavor violating corresponds to the *state selection* models discussed in Ref. [41] as these models also lead to the uniform flavor distribution in the QD limit. To provide a realistic estimate of the potential sensitivity of IceCube to the model parameter space, we also take into account systematic effects described in reference [41] and references therein.

In section 2, we begin by explaining the phenomenological description of QG induced decoherence for a neutrino system, followed by an analysis of the potential to constrain the decoherence parameters for the different models in section 3. Finally, we summarize and discuss our findings in section 4.

## 2 Phenomenological Description of Quantum Gravitational Decoherence in the Neutrino System

Modeling possible effects of interactions of any quantum system with quantum gravitational degrees of freedom (DOFs) without specifying the underlying theory of QG becomes possible in the framework of open quantum systems [13–15, 17, 46]. In that framework, only the dynamics of a subset,  $S$ , of all DOFs is actively considered and the effects due to interactions of this subsystem with the remaining DOFs (usually referred to as *the environment*) are taken into account by introducing unitarity violating terms into the evolution equation of the system. This way the impurity of the state may increase during propagation which is known as decoherence. Therefore, open quantum systems are described using the density operator  $\varrho$  fully characterising the state of the (sub-)system while also allowing for the description of mixed states.

In the following, the DOFs of interest are the neutrino and dark flavors while the environment includes all other DOFs, like for example the matter surrounding the neutrino path as well as hypothetical quantum gravitational DOFs.

Our working hypothesis for these quantum gravitational DOFs can be described as a generalized No-Hair theorem [32, 33]: We assume that in interactions with microscopic black holes from the QG vacuum only unbroken gauge quantum numbers, i.e. color and electric charge, four momentum<sup>1</sup> as well as total angular momentum is conserved while global quantum numbers, such as lepton (family) number, are maximally violated.

This feature makes it necessary to extend the subsystem of neutrino flavors with potentially existing dark fermionic DOFs sharing the same unbroken gauge quantum numbers as neutrinos. Due to the assumed QG behaviour an initially pure neutrino state could then evolve into a mixed state containing non-zero contributions from these dark sectors. This effect could, in principle, be detectable at neutrino telescopes even with atmospheric neutrinos. In this work we analyze and quantify the potential sensitivity of these experiments on constraining QG model parameters with atmospheric neutrinos. To this end, we extend the phenomenological description of this effect from the vacuum case, already extensively discussed in [27, 28], to incorporate all matter effects necessary for a proper description of the propagation of atmospheric neutrinos.

Assuming a memory-less, i.e. Markovian, time evolution, the dynamics of a general open quantum system,  $S$ , are governed by the Lindblad equation [47]:

$$\dot{\varrho}_S = -i[H_S, \varrho_S] + D[\varrho_S]. \quad (1)$$

The first term describes the unitary part of the time evolution due to the system Hamiltonian  $H_S$  as in the usual von Neumann equation for the density operator. The second term, called the dissipator,  $D[\varrho_S]$ , encodes the effective impact of the environmental degrees of freedom on the open system  $S$  and is responsible for the decoherence effect.

Since in the following we consider (ultra relativistic) atmospheric neutrinos propagating through Earth, the Hamiltonian<sup>2</sup> in the vacuum mass basis is given by

$$H_\nu = H_0 + H_{\text{matter}}, \quad \text{with} \quad H_0 = \frac{\Delta M^2}{2E}, \quad \text{and} \quad H_{\text{matter}} = U^\dagger V U, \quad (2)$$

where the mass squared difference matrix is given by  $\Delta M^2 = \text{diag}(0, \Delta m_{21}^2, \dots, \Delta m_{n_f 1}^2)$  with  $\Delta m_{kj}^2 := m_k^2 - m_j^2$ . The number of fermions,  $n_f$ , accounts for the number of active neutrino generations as well as for all dark sectors sharing the same unbroken gauge quantum numbers as the active neutrinos. As we always consider three active generations  $n_f \geq 3$  holds. By choosing the Hamiltonian (2), we implicitly assume that also all other fermions are ultra relativistic at the energy scales of atmospheric neutrinos. This assumption is reasonable assuming that QG interactions approximately conserve the four momentum and hence also the center of mass energy of the propagating system. Therefore only dark sectors with masses within the mass uncertainty of the propagating neutrino wave packets are allowed to appear in the beam. Consequently also the additional particles must have

<sup>1</sup>As spacetime may not be perfectly continuously homogeneous even at very small scales in theories of quantum gravity due to possible pixellation of spacetime, the requirement of four momentum conservation and Lorentz invariance could be relaxed since the theory would not be Poincaré symmetric anymore.

<sup>2</sup>Here we have already subtracted a part proportional to the identity from the Hamiltonian which is allowed since only the commutator of  $H_S$  appears in the Lindblad equation.

masses on the same order of magnitude of the neutrino mass and would propagate at ultra relativistic velocities. If the underlying theory of QG violates energy momentum conservation at high energy scales this reasoning breaks down and also particles with masses outside the mass uncertainty of the neutrino beam can be produced. In this case, it is not guaranteed that the particles appearing in the beam would be ultra relativistic and the corresponding vacuum Hamiltonian entries become

$$\langle \psi_j | H_0 | \psi_j \rangle = \sqrt{\vec{p}^2 + m_{\psi_j}^2} + \delta E_{\text{QG}}, \quad (3)$$

where  $\delta E_{\text{QG}}$  is some potentially Lorentz violating term in the dispersion relation. In the following, we are only interested in flavor transition rates between active neutrino initial and final states. As we assume that mixing between active neutrinos and the dark sector is negligible, the structure of the Lindblad equation (1) ensures that these active-active transition rates are independent of the Hamiltonian components in the dark sector. Therefore, the system Hamiltonian can be assumed to be of the form (2).

Moreover, the matter potential  $V$  in the flavor basis is given by the charged and neutral current neutrino forward scattering potentials in ordinary matter, i.e.

$$V = \text{diag}(V_{\text{CC}} + V_{\text{NC}}, V_{\text{NC}}, V_{\text{NC}}, 0 \dots, 0), \quad (4)$$

and it can be translated to the mass basis using the full mixing matrix of the system

$$U := U_{\text{PMNS}} \oplus \mathbb{I}_{(n_f-3) \times (n_f-3)}, \quad (5)$$

where  $U_{\text{PMNS}}$  is the  $3 \times 3$  Pontecorvo–Maki–Nakagawa–Sakata (PMNS) matrix and we assume that there is little to no a priori mixing of active neutrinos and the dark sector. Of course this framework also applies in case there is non-negligible mixing between these states.

Finally, the dissipator contains several terms due to incoherent scattering of high energy neutrinos with the surrounding matter such as neutrino loss and  $\nu_\tau$  regeneration as described in [48], i.e.

$$D[\varrho_\nu] = D_{\text{matter}}[\varrho_\nu] + D_{\text{QG}}[\varrho_\nu]. \quad (6)$$

Since the matter part of the dissipator is already extensively discussed in the literature [48, 49], we want to focus on the details of  $D_{\text{QG}}[\varrho_\nu]$  from now on. The simplest dissipator respecting the properties of the QG interaction discussed above reads:

$$D_{\text{QG}}[\varrho_\nu] = \sum_{i,j=0}^{n_f^2-1} \mathcal{D}_{\text{QG}}^{i,j} \rho^j \lambda_i \quad \text{with} \quad \mathcal{D}_{\text{QG}} = \text{diag}(0, \Gamma, \dots, \Gamma), \quad (7)$$

where we introduce the usual  $\text{SU}(n_f)$  generator  $\lambda_i$  representation for the density matrix  $\varrho_\nu = \sum_i \rho^i \lambda_i$  and the dissipator. For more details on the choice of basis see appendix A in Ref. [27].

Setting  $\mathcal{D}_{\text{QG}}^{0,j}$  and  $\mathcal{D}_{\text{QG}}^{j,0}$  to zero means that the QG effect does not lead to additional particle loss or creation. Only conversions between different fermion types are permitted. All dissipator elements corresponding to off-diagonal  $\text{SU}(n_f)$  generators damp oscillations while those corresponding to the other diagonal  $\text{SU}(n_f)$  lead to a uniform distribution of the probability across all fermion generations. The oscillation damping effect occurs since QG interactions are assumed to select a certain mass eigenstate while the uniform distribution of probability is required by the maximal flavor violation, i.e. the extended No-Hair theorem discussed above.

The exact expression of the damping factor  $\Gamma$  is unknown since it depends on the details of the underlying theory of QG. However, we can still employ a phenomenological parametrization in terms of the neutrino energy  $E_\nu$ , and consider a representative set of models characterized by how  $\Gamma$  depends on  $E_\nu$ :

$$\Gamma(E_\nu) = \gamma_0 \left( \frac{E_\nu}{E_0} \right)^n. \quad (8)$$

Here,  $n$  is the exponent of the energy,  $E_0$  is a Ref. energy, and  $\gamma_0$  quantifies the strength of the decoherence effect at  $E_0$ . This power-law dependence has been explored in the literature [13–15, 17, 25, 50–52] and considered in

experimental searches [37, 38, 53, 54]. Since QG effects are expected to grow stronger as the wave length of the particles approach the Planck length, it is reasonable to investigate positive values of  $n$  (specifically in the case  $n = 0, 1, 2$ ), but there are also interesting cases where a negative  $n$  dependence arises, see e.g. Ref. [42]. In accordance with the literature, we set  $E_0 = 1 \text{ TeV}$ , to be close to the peak of the neutrino energy distribution observed in the IceCube experiment.

According to Ref. [28] the neutrino oscillation probability in vacuum reads

$$\begin{aligned}
P(\nu_\alpha \rightarrow \nu_\beta) = & \frac{1}{n_f} (1 - \exp(-\Gamma(E_\nu)L)) + \left( \sum_{k=1}^3 |U_{\alpha k}|^2 |U_{\beta k}|^2 \right) \exp(-\Gamma(E_\nu)L) \\
& + 2 \sum_{j>i=1}^3 \text{Re} [U_{\alpha j}^* U_{\alpha i} U_{\beta j} U_{\beta i}^*] \exp \left( -\Gamma(E_\nu)L - \left( \frac{L}{L_{ij}^{\text{coh}}} \right)^2 \right) \cos \left( \frac{\Delta m_{ij}^2 L}{2E_\nu} \right) \\
& - 2 \sum_{j>i=1}^3 \text{Im} [U_{\alpha j}^* U_{\alpha i} U_{\beta j} U_{\beta i}^*] \exp \left( -\Gamma(E_\nu)L - \left( \frac{L}{L_{ij}^{\text{coh}}} \right)^2 \right) \sin \left( \frac{\Delta m_{ij}^2 L}{2E_\nu} \right)
\end{aligned} \tag{9}$$

assuming the dissipator from equation (7) with the baseline  $L$  and  $\Gamma$  as given in equation (8). For the cases  $n \neq 0$ , it is convenient to define the so called coherence energy  $E_{\text{QG}}$ , where

$$\Gamma(E_{\text{QG}})L \stackrel{!}{=} 1 \quad \Leftrightarrow \quad E_{\text{QG}} = E_0 \left( \frac{1}{\gamma_0 L} \right)^{\frac{1}{n}}, \tag{10}$$

indicating the neutrino energy at which the QG effect becomes dominant. Furthermore, we observe that the decoherence effect depends exponentially on the baseline  $L$ , which is why the strongest impact is expected for astrophysical neutrinos, as pointed out in [20]. In the context of astrophysical neutrinos, also the wave packet (WP) separation effect [55–64] becomes significant as the travel distances involved may exceed the coherence length,

$$L_{ij}^{\text{coh}} = 4\sqrt{2}\sigma_x \frac{E_\nu^2}{\Delta m_{ij}^2}, \tag{11}$$

over which the neutrino WPs overlap with each other and coherence is maintained. Here  $\sigma_x$  is the average position space WP width of the neutrino mass eigenstates. This introduces an additional coherence damping exponential<sup>3</sup>  $\exp(-(L/L_{ij}^{\text{coh}})^2)$  as a multiplicative factor in the oscillatory terms in equation (9). Note that WP separation represents only a subleading effect for atmospheric neutrinos and is, hence, neglected in the respective parts of this analysis.

Figure 1 shows the  $\nu_\mu \rightarrow \nu_\mu$  oscillation probability for the exemplary distance of  $L = 14.4 \text{ Mpc}$  to demonstrate the different asymptotic behaviors of the vacuum oscillation probability of astrophysical neutrinos: At low energies the group velocities of the neutrinos are sufficiently different such that the WPs are out of contact by the time they arrive at the detector leading to a constant oscillation probability in the WP decoherence limit. At very high energies the QG decoherence effect dominates damping the oscillation probabilities to  $1/n_f$  as discussed above. It is worth noting that in the QG limit the final flavor ratios of active neutrinos will always be democratic, i.e. (1 : 1 : 1), regardless of the flavor composition at the source.

Depending on the QG and WP parameters there may be also a coherent, oscillatory regime in between the two asymptotic cases. The respective oscillations of the flavor transition probabilities would in principle be observable at neutrino telescopes if the energy resolution is sufficiently high, i.e.

$$\frac{\Delta E_\nu}{E_\nu} \lesssim \frac{2E_\nu}{\Delta m^2 L}, \tag{12}$$

where  $\Delta E_\nu/E_\nu$  is the relative energy resolution of the detector,  $\Delta m^2$  is the mass squared splitting corresponding to the oscillation to be resolved and  $L$  is the distance between neutrino source and detector.

<sup>3</sup>Here we assume Gaussian shaped neutrino wave packets.

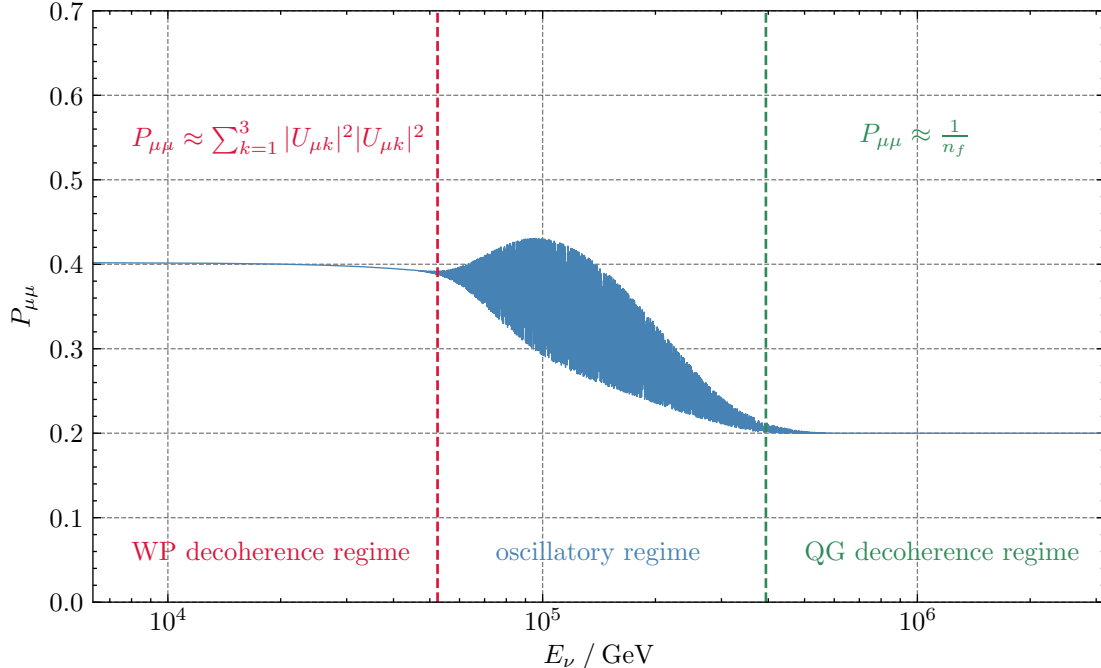


Figure 1: Oscillation probability of  $\nu_\mu \rightarrow \nu_\mu$  for the baseline  $L = 14.4$  Mpc (the distance to NGC 1068), a wave packet width  $\sigma_x = 10^{-9}$  m, the QG parameter  $\gamma_0 = 10^{-35}$  eV, the fermion number of  $n_f = 5$  and the quadratic decoherence model, i.e.  $n = 2$ . The mass squared differences and mixing parameters are extracted from nuFit v5.3 [65, 66] and rounded to the first digit that is not subject to uncertainties.

Despite the superior potential sensitivity of astrophysical neutrinos for QG-induced decoherence the limited statistics of present data makes it difficult to extract reliable constraints (see the discussion in section 3.4). As a result, atmospheric neutrinos currently represent the most suitable candidates for conducting QG searches with positive energy dependence.

### 3 Sensitivity Estimation for the Decoherence Parameter Across All Models

In this section, we assess the potential of the IceCube Neutrino Observatory to detect QG-induced quantum decoherence in the presence of new fermionic particles. The analysis is based on the publicly available Monte Carlo (MC) simulation sample used in Ref. [41] and takes into account all systematic effects discussed in Refs. [41, 67], with no real data used in this work. Firstly, we explain in section 3.1 details of the employed MC sample and how we derive the theory prediction of the various models, before detailing the statistical approach in section 3.2. In section 3.3, we present the expected sensitivities of the IceCube experiment to QG parameters and new particles. Finally, in section 3.4 we discuss potential future analyses aimed at optimising the sensitivity to these parameters.

#### 3.1 Propagation of Fluxes and Detector Response Modelling

To test the model presented in Ref. [27, 28], we focus on high-energy atmospheric neutrinos. In this energy regime, the relevant processes affecting neutrino propagation through the Earth are driven by incoherent scattering of neutrinos with the Earth matter, leading to neutrino absorption [68], energy degradation and tau neutrino regeneration [69, 70]. In order to incorporate all these effects for a given initial neutrino flux, we use

Table 1: A list of all nuisance parameters,  $\eta_j$ , their nominal values, standard deviations and box constraints taken into account in this analysis. For more details see Refs. [41, 67].

Parameter $\eta_j$	Nominal value $\bar{\eta}_j$	Standard Deviation $\sigma_{\eta_j}$	Box constraint
DOM efficiency	0.97	0.1	[0.94, 1.03]
Bulk Ice Gradient 0	0.0	1.0	NA
Bulk Ice Gradient 1	0.0	1.0	NA
Forward Hole Ice ( $p_2$ )	-1.0	10.0	[-5, 3]
Normalization ( $\Phi_{\text{conv.}}$ )	1.0	0.4	NA
Spectral shift ( $\Delta\gamma_{\text{conv.}}$ )	0.00	0.03	NA
Atm. Density	0.0	1.0	NA
Barr WM	0.0	0.40	[-0.5, 0.5]
Barr WP	0.0	0.40	[-0.5, 0.5]
Barr YM	0.0	0.30	[-0.5, 0.5]
Barr YP	0.0	0.30	[-0.5, 0.5]
Barr ZM	0.0	0.12	[-0.25, 0.5]
Barr ZP	0.0	0.12	[-0.2, 0.5]
Normalization ( $\Phi_{\text{astro}}$ )	0.787	0.36	NA
Spectral shift ( $\Delta\gamma_{\text{astro}}$ )	0.0	0.36	NA
Cross section $\sigma_{\nu_\mu}$	1.00	0.03	[0.5, 1.5]
Cross section $\sigma_{\bar{\nu}_\mu}$	1.000	0.075	[0.5, 1.5]
Kaon energy loss $\sigma_{KA}$	0.0	1.0	NA

a modified version of the NuSQuIDS [48] public software, in which we have incorporated an additional decoherence term to account for the potential presence of dark fermionic particles, as described in section 2. As an initial conventional and prompt atmospheric neutrino flux, we use the nuflux package from IceCube [71] for a H3a\_SIBYLL23C model. The astrophysical flux is modelled by a single unbroken power law in neutrino energy with a spectral index of  $-2.5$  [72]. The resulting final flux is then determined for different numbers of fermions  $n_f$  and the different decoherence models. To incorporate the dependence of the decoherence term on the QG parameter  $\gamma_0$ , the final flux is computed and then interpolated across the corresponding  $\gamma_0$  values.

To convert the resulting final fluxes into actual events at IceCube, we use the public MEOWS MC sample [73] and associated tools. These facilitate the transformation from the predicted neutrino flux to detected events, following a similar approach to that described in Ref. [41]. This Monte Carlo release corresponds to  $T = 7.6$  years of livetime. The MC sample contains 24 902 627 unweighted events, which correspond to 305 735 neutrino events weighted within the standard oscillation scenario. The released MEOWS MC dataset consists of only track-like neutrino events, i.e.  $\nu_\mu$  and  $\bar{\nu}_\mu$ , whose available information are the true and reconstructed energy and cosine of the zenith angle. The reconstruction achieves an energy resolution of  $\sigma_{\log_{10}(E_{\nu_\mu})} \sim 0.3$  and an angular resolution  $\sigma_{\cos\theta_{\text{zenith}}}$  between 0.005 and 0.015 as a function of the energy [67].

In order to incorporate the new decoherence effects we reweight the MC events with the appropriate oscillation probabilities evaluated with NuSQuIDS. We also take into account the systematic effects of the detector and the initial flux models by allowing for an additional, dynamical rescaling of the MC weights depending on the set of nuisance parameters  $\vec{\eta}$  described in Refs. [41, 67] and listed in table 1.

### 3.2 Statistical Approach

To estimate the constraints that neutrino oscillation experiments can place on the QG-parameter  $\gamma_0$ , we conduct a likelihood ratio test on the binned, reweighted MC event counts. In order to correctly take into account all relevant systematic effects as well as MC modeling uncertainties in the analysis of the counting experiment under consideration, we employ a profile likelihood function that is given by a product of a likelihood describing the

bin counts,  $\mathcal{L}_{\text{bin}}$ , and a penalty term,  $\Pi(\vec{\eta})$ , encoding the distribution information of the nuisance parameters  $\vec{\eta}$ . For a given data set,  $\vec{X}$ , and a chosen decoherence model, i.e. for fixed  $n_f$  and  $n$ , the profile likelihood function is then obtained by maximizing over the set of nuisance parameters:

$$\mathcal{L}_{\text{profile}}(\gamma_0|\vec{X}) := \sup_{\vec{\eta}} \mathcal{L}_{\text{bin}}(\gamma_0, \vec{\eta}|\vec{X})\Pi(\vec{\eta}). \quad (13)$$

We model the nuisance penalty term,

$$\Pi(\vec{\eta}) = \prod_{j=1}^{N_{\text{sys}}} \frac{e^{-\frac{(\eta_j - \bar{\eta}_j)^2}{2\sigma_{\eta_j}^2}}}{\sqrt{2\pi\sigma_{\eta_j}^2}}, \quad (14)$$

as a product of independent, one-dimensional normal distributions, with nominal values,  $\bar{\eta}_j$ , and standard deviations,  $\sigma_{\eta_j}$ , taken from reference [67] and specified in table 1.

The likelihood function describing the distribution of bin counts is taken as [74],

$$\mathcal{L}(\gamma_0, \vec{\eta}|\vec{X}) = \prod_{l=1}^{n_{\text{bins}}} \mathcal{L}_{\text{eff}}(n_{\mu,l}(\gamma_0, \vec{\eta}), \sigma_l(\gamma_0, \vec{\eta})|X_l), \quad (15)$$

where  $n_{\text{bins}}$  is the total number of bins and  $X_l$  is the measured number of events in bin  $l$ . Furthermore, the expected number of event counts,  $n_{\mu,l}(\gamma_0, \vec{\eta})$ , and the associated MC uncertainty,  $\sigma_{\text{MC},l}^2(\gamma_0, \vec{\eta})$ , in bin  $l$  predicted according to a given decoherence model are computed from the MC weights,  $\omega_i^l$ , as follows:

$$n_{\mu,l}(\gamma_0, \vec{\eta}) = \sum_{i=1}^{N_l} \omega_i^l(\gamma_0, \vec{\eta}), \quad \sigma_{\text{MC},l}^2(\gamma_0, \vec{\eta}) = \sum_{i=1}^{N_l} [\omega_i^l(\gamma_0, \vec{\eta})]^2. \quad (16)$$

Here, the  $i$ -summation runs over all weights associated to the  $l$ -th bin. The bin-wise likelihood function  $\mathcal{L}_{\text{eff}}$  is an adaption of the Poisson likelihood, specifically designed to account for statistical uncertainties from MC simulations, first introduced in reference [74].

The logarithmic likelihood ratio test statistic is then defined as

$$\ln \Lambda := -2 \ln \left( \frac{\sup_{\gamma_0 \in \Theta_0} \mathcal{L}_{\text{profile}}(\gamma_0|\vec{X})}{\sup_{\gamma_0 \in \Theta} \mathcal{L}_{\text{profile}}(\gamma_0|\vec{X})} \right), \quad (17)$$

where the parameter space of the null hypothesis,  $\Theta_0 = \{\gamma_0^0\}$ , consists of a single parameter configuration that we wish to test. As the toy data set, we take the prediction of the standard case, i.e.  $X_i = n_{\mu,i}^{\text{std}} := n_{\mu,i}(\gamma_0 = 0, \vec{\eta})$ . For  $\gamma_0 = 0$  the event counts in each bin are independent of the number of fermions  $n_f$  and energy dependence  $n$  of the decoherence model. The full parameter space,  $\Theta$ , for each combination  $(n_f, n)$  in the null hypothesis can be taken as  $\Theta = \mathbb{R}$ . Thus, for a given choice  $(n_f, n)$  we perform a one dimensional likelihood ratio test for the QG parameter  $\gamma_0$ .

In the limit of large event counts, the log likelihood ratio converges to the following, simple  $\chi^2$  test statistic:

$$\ln \Lambda(\gamma_0) \rightarrow \chi^2(\gamma_0) = \min_{\vec{\eta}} \sum_{l=1}^{n_{\text{bins}}} \frac{(n_{\mu,l}^{\text{std}} - n_{\mu,l}(\gamma_0, \vec{\eta}))^2}{n_{\mu,l}(\gamma_0, \vec{\eta}) + \sigma_{\text{MC},l}^2(\gamma_0, \vec{\eta})} + \sum_{j=1}^{N_{\text{sys}}} \frac{(\eta_j - \bar{\eta}_j)^2}{\sigma_{\eta_j}^2}. \quad (18)$$

According to Wilk's theorem  $\ln(\Lambda)$  follows a  $\chi^2$  distribution with one DOF since  $\Theta_0 \subset \text{interior}(\Theta)$  and the large event count limit applies to good approximation. This allows us to specify the confidence levels (C.L.s) of the  $\gamma_0$  exclusion limits by comparing the respective  $\chi^2(\gamma_0)$  value to the threshold values of the  $\chi^2$  distribution.

### 3.3 Expected Sensitivities for the IceCube Neutrino Observatory

In this section, we determine the expected potential of the IceCube experiment to probe the QG parameters presented in this work. Figure 2 presents the dependence of  $\chi^2$  on the decoherence parameter  $\gamma_0$  for the



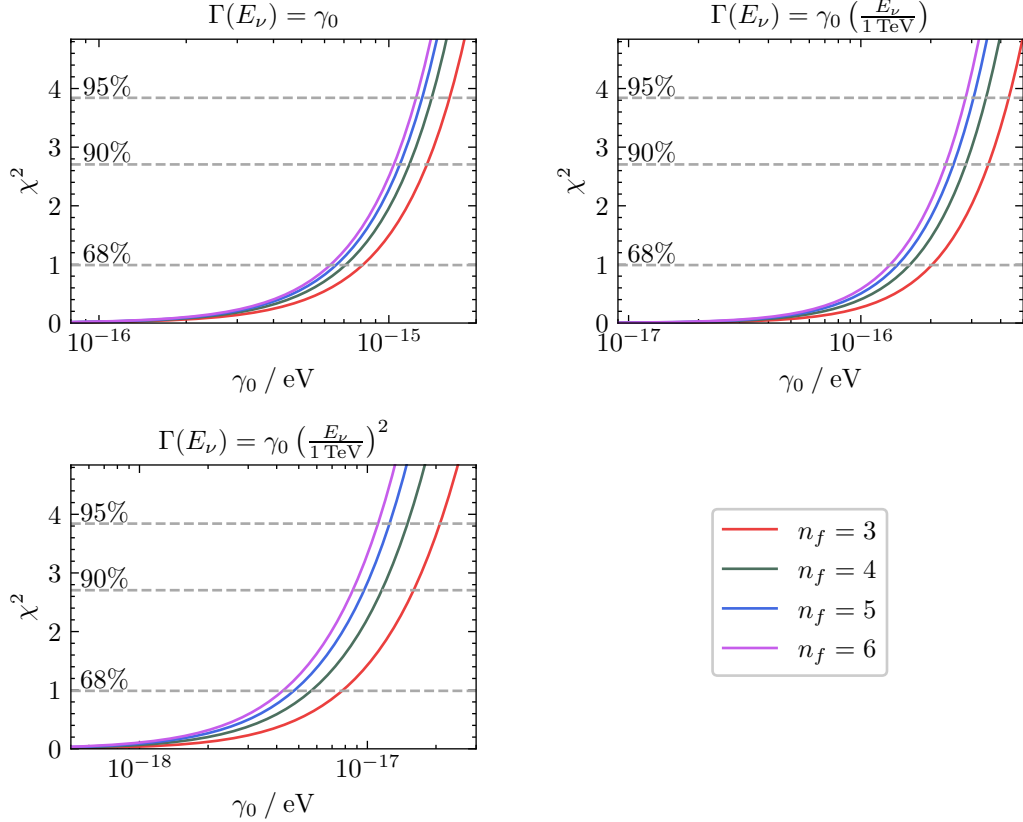


Figure 2: Estimated IceCube sensitivity for  $T = 7.6$  years of livetime, for the three decoherence models under consideration, each with varying fermion numbers. The  $\chi^2$  threshold values for the 68%, 90% and 95% C.L.s are also reported as dashed lines.

Table 2: The  $\gamma_0/\text{eV}$  values at 90% C.L. for the different energy dependencies and  $n_f \in \{3, 4, 5, 6\}$ . In parentheses we report the idealized bounds obtained in a statistics-only approach, i.e. neglecting systematic effects.

$n_f$	$\Gamma(E_\nu)$		
	$\gamma_0$	$\gamma_0 \left(\frac{E_\nu}{1\text{TeV}}\right)$	$\gamma_0 \left(\frac{E_\nu}{1\text{TeV}}\right)^2$
3	$1.35 \times 10^{-15}$ ( $1.52 \times 10^{-16}$ )	$3.54 \times 10^{-16}$ ( $5.20 \times 10^{-17}$ )	$1.60 \times 10^{-17}$ ( $2.76 \times 10^{-18}$ )
4	$1.18 \times 10^{-15}$ ( $1.33 \times 10^{-16}$ )	$2.83 \times 10^{-16}$ ( $4.37 \times 10^{-17}$ )	$1.16 \times 10^{-17}$ ( $2.11 \times 10^{-18}$ )
5	$1.09 \times 10^{-15}$ ( $1.24 \times 10^{-16}$ )	$2.51 \times 10^{-16}$ ( $3.99 \times 10^{-17}$ )	$9.68 \times 10^{-18}$ ( $1.81 \times 10^{-18}$ )
6	$1.04 \times 10^{-15}$ ( $1.18 \times 10^{-16}$ )	$2.32 \times 10^{-16}$ ( $3.76 \times 10^{-17}$ )	$8.63 \times 10^{-18}$ ( $1.65 \times 10^{-18}$ )

various decoherence models discussed in section 2, differing in their energy-dependence,  $n$ , and in the number of fermions,  $n_f$ . The 68%, 90% and 95% C.L.s are indicated by dashed lines. Table 2 reports the 90% C.L. values for the QG parameter  $\gamma_0$  for the different energy dependencies which are, for  $n_f = 3$ , in good agreement with the literature [41]. In addition to the bounds obtained taking into account systematic effects of the experiment, we also show the equivalent bounds derived from a statistics-only approach in Table 2. This comparison provides an estimate of the impact of systematic uncertainties. The analysis shows that the sensitivity to the QG parameter strengthens, as the number of fermions increases, which aligns with expectations. This behavior is anticipated because the decoherence limit diverges from the standard case with an increasing number of fermions,

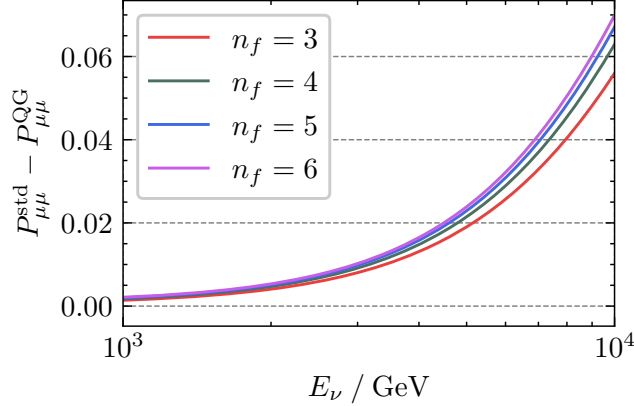


Figure 3: Difference between the standard and QG model prediction of the  $\nu_\mu \rightarrow \nu_\mu$  transition probability,  $P_{\mu\mu}^{\text{std}}$  and  $P_{\mu\mu}^{\text{QG}}$ , for various numbers of fermions in the quadratic decoherence model, with  $\cos\theta_{\text{zenith}} = -1$ , corresponding to a baseline equal to the Earth diameter. Here, the model probabilities are evaluated at the 95% C.L.  $\gamma_0 = 2.08 \times 10^{-17}$  eV for  $n_f = 3$  and  $n = 2$ .

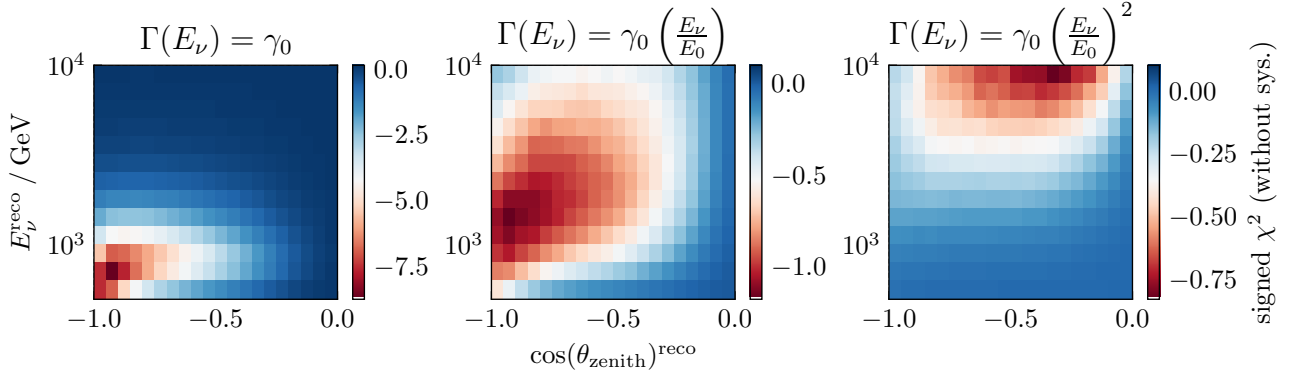


Figure 4: Signed  $\chi^2$  values (without systematic effects) for  $n_f = 4$  and the three energy dependencies as a function of the reconstructed zenith angle  $\cos(\theta_{\text{zenith}})^{\text{reco}}$  and reconstructed energy  $E_\nu^{\text{reco}}$ , corresponding to the 95% C.L.  $\gamma_0$  values:  $\gamma_0 \in \{1.41 \times 10^{-15}, 3.46 \times 10^{-16}, 1.50 \times 10^{-17}\}$  eV (from left to right).

as illustrated in Figure 3. Moreover, the bounds become more stringent as the power of the energy dependence in the decoherence model increases. Considering Figure 3, we see that for an energy-dependent decoherence model the largest deviation is expected in high-energy neutrinos. At the 95% C.L. bounds determined in this analysis the difference to the standard  $\nu_\mu \rightarrow \nu_\mu$  probability is about 6% at  $E_\nu \sim 10$  TeV.

To further explore the relevant energy and cosine zenith regions that contribute to the IceCube sensitivity, we use the signed  $\chi^2$  values per bin defined by

$$\text{signed } \chi_l^2 = \frac{(n_{\mu,l}^{\text{QG}} - n_{\mu,l}^{\text{std}}) |n_{\mu,l}^{\text{QG}} - n_{\mu,l}^{\text{std}}|}{n_{\mu,l}^{\text{QG}}}, \quad (19)$$

where  $n_{\mu,l}^{\text{QG}}$  are the binned number of events for the respective model with a fixed QG parameter  $\gamma_0$  and  $n_{\mu,i}^{\text{std}}$  are the binned number of events in the standard case. Figure 4 presents the signed  $\chi^2$  computed from the nominal MC weights, i.e. without taking into account systematic effects, for  $n_f = 4$  and the different decoherence models as a function of reconstructed zenith angle  $\cos\theta_{\text{zenith}}^{\text{reco}}$  and reconstructed energy  $E_\nu^{\text{reco}}$ , for  $\gamma_0$  such that  $\chi^2 = 3.85$ , corresponding to the 95% CL, and the respective  $\gamma_0$ . As a cross-check, Figure 5 shows an analogous quantity representing the binned true  $\nu_\mu$  fluxes. Comparing both Figures we can see that the effect of

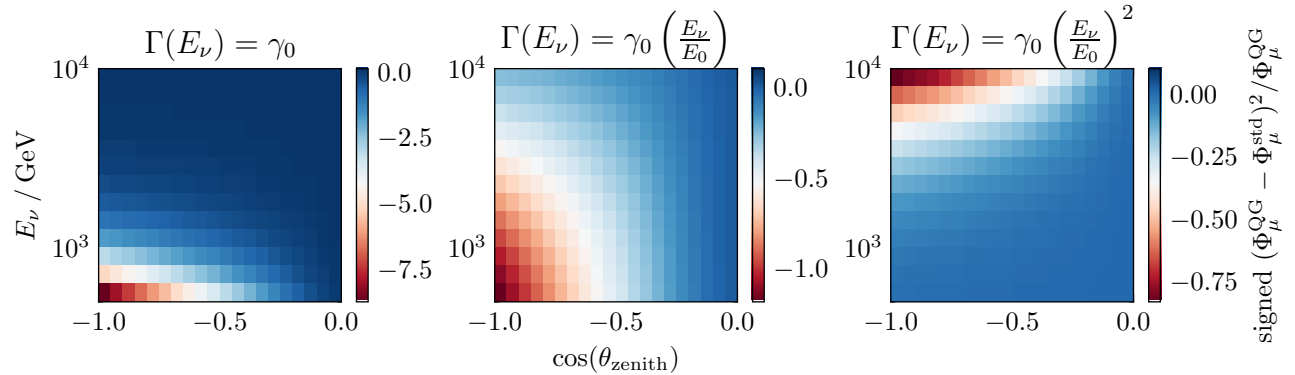


Figure 5: Cross-checks for the signed  $\chi^2$  distributions ( $n_f = 4$ ) in terms of the binned, true  $\nu_\mu$  fluxes in the energy  $E_\nu$  and cosine zenith angle  $\cos(\theta_{\text{zenith}})$  plane, scaled such that the minimum of the shown quantity and that of the associated signed  $\chi^2$  match. Each panel corresponds to a different energy dependence of the underlying QG model, i.e.  $n \in \{0, 1, 2\}$  (from left to right) and the associated 95% C.L. bounds  $\gamma_0 \in \{1.41 \times 10^{-15}, 3.46 \times 10^{-16}, 1.50 \times 10^{-17}\}$  eV.

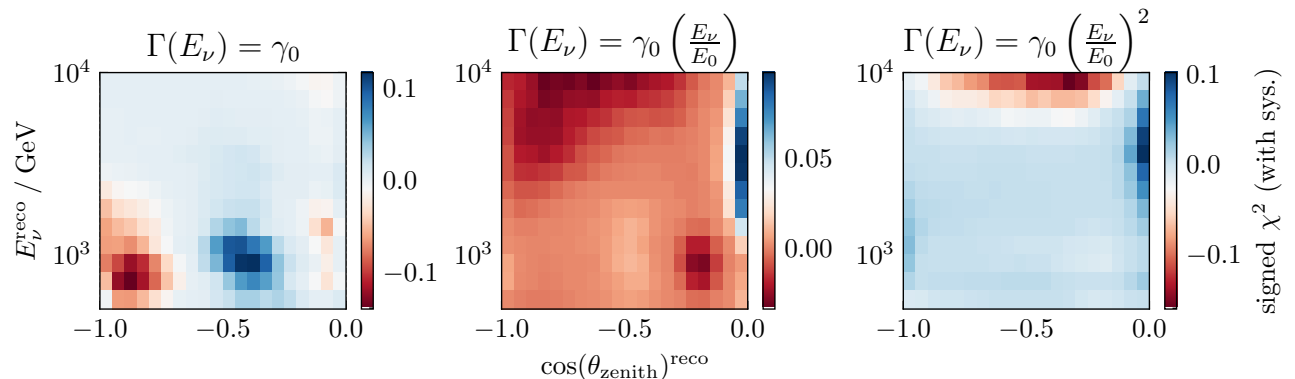


Figure 6: Signed  $\chi^2$  values (with systematic effects) for  $n_f = 4$  and the three energy dependencies as a function of the reconstructed zenith angle  $\cos(\theta_{\text{zenith}})^{\text{reco}}$  and reconstructed energy  $E_\nu^{\text{reco}}$ , corresponding to the 95% C.L.  $\gamma_0$  values:  $\gamma_0 \in \{1.41 \times 10^{-15}, 3.46 \times 10^{-16}, 1.50 \times 10^{-17}\}$  eV (from left to right).

energy and directional reconstruction on average results in a shift of the regions of highest sensitivity to higher reconstructed energies and cosine zenith values. From the sensitivity distribution in terms of the true energy and cosine zenith it can be observed that, in the case of  $\Gamma(E) \equiv \gamma_0$ , the highest sensitivities are expected in the region of lower cosine zenith, corresponding to up-going events, and lower energies. The latter is explained by the much higher statistics in the low energy bins compared to the high energy bins. In contrast, for the other energy-dependent decoherence models, the sensitivity shifts to higher energies as the impact of the QG effect increases in the high-energy bins.

In order to estimate how the systematic effects impact the regions of highest sensitivity, we also compute the signed  $\chi^2$  values from the rescaled MC events at the corresponding best fit value of the nuisance parameter vector  $\vec{\eta}$  obtained from the profile likelihood procedure. This quantity is shown in Figure 6 again for  $n_f = 4$  and the different energy dependencies as a function of the reconstructed cosine zenith and energy. From the comparison of the signed  $\chi^2$  distributions with and without systematic effects, i.e. Figures 6 and 4, we observe that the systematic effects can induce significant deviations between the naively expected and the actual regions of highest sensitivity. Across all decoherence models we see that the overall sensitivity is drastically reduced due to the rescaling of the nominal MC weights which is of course expected as we minimize  $\chi^2$  on the set of nuisance parameters. For the energy-independent decoherence model, i.e.  $n = 0$ , we still see that the largest (negative)

deviation of signed  $\chi^2$ , caused by the model effects, is located in the up-going, low-energy bins as expected, but we also find a region of positive deviation caused by the application of bin-wise scale factors describing the systematic effects after minimizing  $\chi^2$  with respect to the set of nuisance parameters. In case of the  $n = 1$  decoherence model, we find that after applying the systematic effects at the best fit point  $\vec{\eta} = \vec{\eta}_{\text{opt}}$ , the region of maximal sensitivity is further smeared across all energy and cosine zenith bins. Lastly, for the quadratically energy-dependent decoherence model, as in the case  $n = 0$ , the region of highest sensitivity remains mostly intact compared to the corresponding region shown in Figure 4.

### 3.4 Future prospects

As discussed in section 2, astrophysical neutrinos are ideal candidates for this analysis due to their longer baselines and higher energies compared to atmospheric neutrinos. However, this approach is currently impractical due to limited statistics. Ref. [75] presents the results of a nine-year (2011–2020) time-integrated analysis of IceCube data, identifying three astrophysical neutrino sources with higher statistical local significance (pre-trial): NGC 1068 with 79 signal events at  $5.2\sigma$ , PKS 1424+240 with 77 signal events at  $3.7\sigma$ , and TXS 0506+056 with 5 signal events at  $3.5\sigma$ .

Among the cited sources, NGC 1068 is particularly interesting due to the relatively narrow energy range of the detected events, concentrated in the  $\sim [1, 10]$  TeV region. Figure 7 shows the ratio of the expected flux from NGC 1068 in the QG scenario, normalized to the standard flux  $\Phi_{\text{tot}}^{\text{std}}$ , for neutrino energies within the  $[1, 10]$  TeV region and for  $E_{\text{QG}} = 5$  TeV, c.f. equation (10). We model the flux of neutrino flavor  $\alpha$  at Earth as  $\phi_{\alpha}^{\text{Earth}} := \sum_{\beta} P_{\beta\alpha} \phi_{\beta}^{\text{source}}$  and the total flux as  $\phi_{\text{tot}} := \sum_{\alpha} \phi_{\alpha}^{\text{Earth}}$ , where  $P_{\beta\alpha}$  is the  $\nu_{\beta} \rightarrow \nu_{\alpha}$  flavor transition probability. Moreover, we model the source flux<sup>4</sup> of neutrino flavor  $\nu_{\alpha}$ ,  $\phi_{\alpha}^{\text{source}} := c_{\alpha} \Phi_0 E^{-\sigma}$ , as a simple power-law spectrum with spectral index  $\sigma$ , common amplitude  $\Phi_0$  and initial flavor ratios  $c_{\alpha}$  normalized such that  $1 = \sum_{\alpha} c_{\alpha}$ . The flux ratio,  $\Phi_{\text{tot}}^{\text{QG}} / \Phi_{\text{tot}}^{\text{std}}$ , shown in Figure 7 is therefore independent of  $\Phi_0$ ,  $\sigma$  and the initial flavor ratio  $c_{\alpha}$  under these assumptions. Note that  $\Phi_{\text{tot}}^{\text{QG}} / \Phi_{\text{tot}}^{\text{std}}$  represents a purely theoretical quantity used to emphasize how the QG model differs from the standard prediction given the same initial flux spectrum. This however cannot be used to analyze an actual data set since both the standard and QG predictions need to be fitted to the data individually resulting in possibly different parameter values  $\Phi_0$ ,  $\sigma$ , and so on.

If  $E_{\text{QG}}$  is located within or close to the interval of observed neutrino energies, a prominent dip towards the asymptotic limit  $\phi_{\text{tot}}^{\text{QG}} \rightarrow 3/n_f \phi_{\text{tot}}^{\text{std}}$  can be observed, c.f. Figure 7. This characteristic could allow for an energy-dependent QD analysis. However, such an analysis would likely need to be model-dependent, assuming the currently fitted spectrum is correct. For a more realistic and model-independent analysis, where different spectral models, source flavor compositions, and additional quantum decoherence parameters are simultaneously fitted, the current available statistics are insufficient to achieve a statistically significant result.

If  $E_{\text{QG}} > E_{\text{max}}$ , where  $E_{\text{min}}/E_{\text{max}}$  are the lower and upper boundaries of the observed energy region, QG-induced decoherence has not yet become dominant. In this case, the QG fluxes approximately match the standard prediction. The last possible scenario,  $E_{\text{QG}} < E_{\text{min}}$ , corresponds to the case where the system is already in the QD limit and the total flux reached its asymptotic value,  $\phi_{\text{tot}}^{\text{QG}} = 3/n_f \phi_{\text{tot}}^{\text{std}}$ . Thus the QD effect would only result in a rescaling of the flux normalization and could not be estimated separately by fitting the neutrino fluxes.

The number of events collected per source and the required observation years indicate that it will take a significant amount of time before an astrophysical analysis can place meaningful constraints on these parameters.

In this respect, in the coming years, it may be beneficial to conduct a combined atmospheric neutrino analysis between IceCube and KM3NeT. Such an analysis would not only benefit from the additional statistics provided by KM3NeT but also from the different systematics affecting the analysis, enabling stronger statistical constraints on the quantum decoherence parameters.

On the KM3NeT side, ARCA would be the most suitable detector for this analysis; however, ORCA could also be employed, particularly for the energy-independent QD model. In Figure 8, we show the expected deviations of neutrino fluxes from standard predictions under the constant decoherence model ( $\Gamma = \gamma_0$ ), as the

<sup>4</sup>To be precise, the quantity  $\phi_{\alpha}^{\text{source}}$  describes the expected flux of neutrino flavor  $\nu_{\alpha}$  at Earth if neutrinos did not oscillate. Therefore, it maintains the initial energy spectrum and flavor composition but also takes into account the spreading of the neutrino beam.

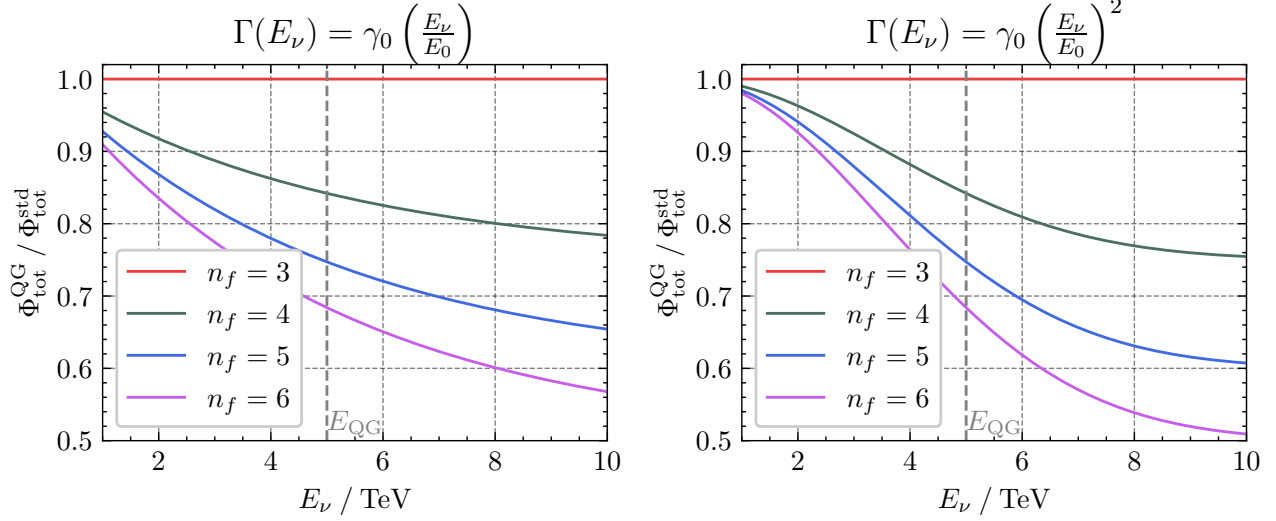


Figure 7: Total flux  $\Phi_{\text{tot}}^{\text{QG}}$  normalized to the total standard flux  $\Phi_{\text{tot}}^{\text{std}}$  for  $L = 14.4$  Mpc for the  $n = 1$  and  $n = 2$  decoherence models in the case of  $E_{\text{min}} < E_{\text{QG}} = 5 \text{ TeV} < E_{\text{max}}$  and for an initial  $(1 : 2 : 0)$  neutrino flavor ratio.

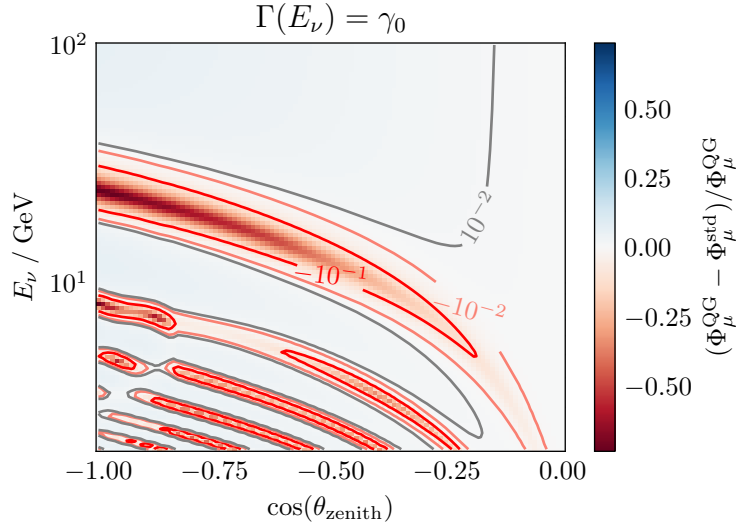


Figure 8: Muon neutrino oscillogram for  $n_f = 4$  in case of the constant decoherence model and for the corresponding 95% C.L.  $\gamma_0 = 1.41 \times 10^{-15} \text{ eV}$  value. Shown is the relative muon neutrino flux deviation as a function of the energy  $E_\nu$  and the zenith angle  $\cos \theta_{\text{zenith}}$ .

models with positive energy dependence are not relevant in the low-energy regime, and assuming a fermion number of  $n_f = 4$ . The plot suggests that we anticipate the signal to be within the energy range below 20 GeV, with a particular focus on below 10 GeV. This is the energy region for which ORCA is specifically optimised. Additionally, an analysis using DeepCore [76] would also be feasible, as it has an energy threshold of about 10 GeV. Plots for ARCA are not shown as the expected signal region is similar to the IceCube one (see Figure 5).

## 4 Summary and Discussion

This work examines the impact of Quantum Gravity (QG) on atmospheric neutrino oscillations, considering the presence of additional hypothetical dark fermions. Since we do not assume an underlying theory of QG, we adopt an effective description in the framework of open quantum systems. This is based on the assumption that neutrino flavor eigenstates become entangled with unknown QG degrees of freedom (DOFs) during propagation. Since these DOFs can not be directly probed with current experimental methods, only the flavor subsystem is observable. Consequently, decoherence arises in the neutrino flavor subsystem due to the entanglement between the observed and unobserved DOFs.

A central assumption in this analysis is that QG maximally violates the conservation of quantum numbers associated with global symmetries and that it only conserves unbroken gauge quantum numbers as well as angular momentum and energy. Due to the aforementioned decoherence effect an initially pure neutrino beam could then develop a non-zero component of potentially existing dark fermions. Since QG is assumed to maximally violate conservation of lepton flavor in the asymptotic limit all transition probabilities must approach  $1/n_f$ , where  $n_f \geq 3$  is the total number of fermions. Possible candidates for dark fermions are WIMPs [34], sterile neutrinos [35], and FIMPS [36].

We consider several decoherence models differing only in the dependence of the decoherence parameter,  $\Gamma \propto \gamma_0 E_\nu^n$ , on the neutrino energy  $E_\nu$  with power-law  $n$  and the total number of dark fermions  $n_f$  determining the dimension of flavor space. A statistical analysis, based on publicly available Monte Carlo (MC) simulations, has been performed to determine the expected potential of the IceCube Neutrino Observatory to probe the QG parameter  $\gamma_0$ . The expected sensitivities have been determined by reweighting the public MC sample provided by IceCube taking into account the new decoherence effects as well as the systematic effects caused by the detector response and the initial neutrino flux model. The analysis also determines the specific energy ranges and zenith angles where sensitivities could be anticipated for IceCube.

The analysis was conducted for various total numbers of dark fermions. The results confirm the expectation that the sensitivity increases with a higher number of fermions. This demonstrates that, under the model assumptions, atmospheric neutrino experiments can in principle be used to discriminate between different new physics scenarios involving different numbers of dark fermions. Moreover, combining astrophysical with atmospheric neutrino data can lead to further improvements potentially allowing for a simultaneous fit of all model parameters, including the number of fermion generations  $n_f$ , as astrophysical neutrinos are even more sensitive to the QG effect due to their orders of magnitude larger travel distances.

However, the currently limited statistics do not allow for a comprehensive analysis. Meanwhile, combining atmospheric neutrino data from IceCube and KM3NeT detectors would be promising. Integrating data from both experiments would enhance the statistical power and address different systematic uncertainties, ultimately leading to a stronger potential for probing the QG parameters.

## Acknowledgements

A. Domi acknowledges the support from the European Union’s Horizon 2021 research and innovation programme under the Marie Skłodowska-Curie grant agreement No. 101068013 (QGRANT).

## References

- [1] A. Addazi et al., *Quantum gravity phenomenology at the dawn of the multi-messenger era—A review*, *Prog. Part. Nucl. Phys.* **125** (2022) 103948, [2111.05659].
- [2] J. Polchinski, *String theory. Vol. 1: An introduction to the bosonic string*. Cambridge Monographs on Mathematical Physics. Cambridge University Press, 12, 2007, 10.1017/CBO9780511816079.
- [3] K. Becker, M. Becker and J. H. Schwarz, *String theory and M-theory: A modern introduction*. Cambridge University Press, 12, 2006, 10.1017/CBO9780511816086.
- [4] L. E. Ibanez and A. M. Uranga, *String theory and particle physics: An introduction to string phenomenology*. Cambridge University Press, 2, 2012.
- [5] C. Rovelli and L. Smolin, *Knot Theory and Quantum Gravity*, *Phys. Rev. Lett.* **61** (1988) 1155.
- [6] C. Rovelli and L. Smolin, *Loop Space Representation of Quantum General Relativity*, *Nucl. Phys. B* **331** (1990) 80–152.
- [7] C. Rovelli and L. Smolin, *Discreteness of area and volume in quantum gravity*, *Nucl. Phys. B* **442** (1995) 593–622, [gr-qc/9411005].
- [8] A. Ashtekar, *Gravity and the quantum*, *New J. Phys.* **7** (2005) 198, [gr-qc/0410054].
- [9] T. Thiemann, *Loop Quantum Gravity: An Inside View*, *Lect. Notes Phys.* **721** (2007) 185–263, [hep-th/0608210].
- [10] M. Celada, D. González and M. Montesinos, *BF gravity*, *Class. Quant. Grav.* **33** (2016) 213001, [1610.02020].
- [11] C. Kiefer, *Conceptual Problems in Quantum Gravity and Quantum Cosmology*, *ISRN Math. Phys.* **2013** (2013) 509316, [1401.3578].
- [12] S. W. Hawking, *The Unpredictability of Quantum Gravity*, *Commun. Math. Phys.* **87** (1982) 395–415.
- [13] J. R. Ellis, J. S. Hagelin, D. V. Nanopoulos and M. Srednicki, *Search for Violations of Quantum Mechanics*, *Nucl. Phys. B* **241** (1984) 381.
- [14] J. R. Ellis, N. E. Mavromatos and D. V. Nanopoulos, *Testing quantum mechanics in the neutral kaon system*, *Phys. Lett. B* **293** (1992) 142–148, [hep-ph/9207268].
- [15] P. Huet and M. E. Peskin, *Violation of CPT and quantum mechanics in the  $K^0$  - anti- $K^0$  system*, *Nucl. Phys. B* **434** (1995) 3–38, [hep-ph/9403257].
- [16] Y. Liu, J.-L. Chen and M.-L. Ge, *A Constraint on EHNS parameters from solar neutrino problem*, *J. Phys. G* **24** (1998) 2289–2296, [hep-ph/9711381].
- [17] C.-H. Chang, W.-S. Dai, X.-Q. Li, Y. Liu, F.-C. Ma and Z.-j. Tao, *Possible effects of quantum mechanics violation induced by certain quantum gravity on neutrino oscillations*, *Phys. Rev. D* **60** (1999) 033006, [hep-ph/9809371].
- [18] F. Benatti and R. Floreanini, *Open system approach to neutrino oscillations*, *JHEP* **02** (2000) 032, [hep-ph/0002221].
- [19] A. M. Gago, E. M. Santos, W. J. C. Teves and R. Zukanovich Funchal, *A Study on quantum decoherence phenomena with three generations of neutrinos*, hep-ph/0208166.
- [20] H. V. Klapdor-Kleingrothaus, H. Päs and U. Sarkar, *Effects of quantum space-time foam in the neutrino sector*, *Eur. Phys. J. A* **8** (2000) 577–580, [hep-ph/0004123].

- [21] D. Hooper, D. Morgan and E. Winstanley, *Probing quantum decoherence with high-energy neutrinos*, *Phys. Lett. B* **609** (2005) 206–211, [[hep-ph/0410094](#)].
- [22] D. Hooper, D. Morgan and E. Winstanley, *Lorentz and CPT invariance violation in high-energy neutrinos*, *Phys. Rev. D* **72** (2005) 065009, [[hep-ph/0506091](#)].
- [23] L. A. Anchordoqui, H. Goldberg, M. C. Gonzalez-Garcia, F. Halzen, D. Hooper, S. Sarkar et al., *Probing Planck scale physics with IceCube*, *Phys. Rev. D* **72** (2005) 065019, [[hep-ph/0506168](#)].
- [24] G. Barenboim, N. E. Mavromatos, S. Sarkar and A. Waldron-Lauda, *Quantum decoherence and neutrino data*, *Nucl. Phys. B* **758** (2006) 90–111, [[hep-ph/0603028](#)].
- [25] T. Stuttard and M. Jensen, *Neutrino decoherence from quantum gravitational stochastic perturbations*, *Phys. Rev. D* **102** (2020) 115003, [[2007.00068](#)].
- [26] H. D. Zeh, *On the interpretation of measurement in quantum theory*, *Found. Phys.* **1** (1970) 69–76.
- [27] D. Hellmann, H. Päs and E. Rani, *Searching new particles at neutrino telescopes with quantum-gravitational decoherence*, *Phys. Rev. D* **105** (2022) 055007, [[2103.11984](#)].
- [28] D. Hellmann, H. Päs and E. Rani, *Quantum gravitational decoherence in the three neutrino flavor scheme*, *Phys. Rev. D* **106** (2022) 083013, [[2208.11754](#)].
- [29] L. A. Anchordoqui, *Spacetime foam at a TeV*, *J. Phys. Conf. Ser.* **60** (2007) 191–194, [[hep-ph/0610025](#)].
- [30] E. Witten, *Symmetry and Emergence*, *Nature Phys.* **14** (2018) 116–119, [[1710.01791](#)].
- [31] D. Harlow and H. Ooguri, *Constraints on Symmetries from Holography*, *Phys. Rev. Lett.* **122** (2019) 191601, [[1810.05337](#)].
- [32] S. W. Hawking, *Particle Creation by Black Holes*, *Commun. Math. Phys.* **43** (1975) 199–220.
- [33] D. N. Page, *Particle Transmutations in Quantum Gravity*, *Phys. Lett. B* **95** (1980) 244–246.
- [34] L. Roszkowski, E. M. Sessolo and S. Trojanowski, *WIMP dark matter candidates and searches—current status and future prospects*, *Rept. Prog. Phys.* **81** (2018) 066201, [[1707.06277](#)].
- [35] B. Dasgupta and J. Kopp, *Sterile Neutrinos*, *Phys. Rept.* **928** (2021) 1–63, [[2106.05913](#)].
- [36] S. Westhoff, *FIMP Dark Matter at the LHC*, *PoS LHCP2023* (2024) 221, [[2312.13373](#)].
- [37] A. L. G. Gomes, R. A. Gomes and O. L. G. Peres, *Quantum decoherence and relaxation in long-baseline neutrino data*, *JHEP* **10** (2023) 035, [[2001.09250](#)].
- [38] P. Coloma, J. Lopez-Pavon, I. Martinez-Soler and H. Nunokawa, *Decoherence in Neutrino Propagation Through Matter, and Bounds from IceCube/DeepCore*, *Eur. Phys. J. C* **78** (2018) 614, [[1803.04438](#)].
- [39] KM3NeT Collaboration, *Search for Quantum Decoherence in Neutrino Oscillations with KM3NeT ORCA6*, *PoS ICRC2023* (2023) 1025.
- [40] V. De Romeri, C. Giunti, T. Stuttard and C. A. Ternes, *Neutrino oscillation bounds on quantum decoherence*, *Journal of High Energy Physics* **2023** (Sept., 2023) .
- [41] IceCube Collaboration, *Search for decoherence from quantum gravity with atmospheric neutrinos*, *Nature Phys.* **20** (2024) 913–920.
- [42] A. Domi, T. Eberl, M. J. Fahn, K. Giesel, L. Hennig, U. Katz et al., *Understanding gravitationally induced decoherence parameters in neutrino oscillations using a microscopic quantum mechanical model*, [2403.03106](#).



- [43] IceCube Collaboration, *The icecube neutrino observatory: instrumentation and online systems*, *Journal of Instrumentation* **12** (Mar., 2017) P03012–P03012.
- [44] ANTARES Collaboration, *Legacy results of the ANTARES Neutrino Telescope*, *PoS EPS-HEP2023* (2023) 061.
- [45] KM3NeT Collaboration, *Letter of intent for KM3NeT 2.0*, *J. Phys. G* **43** (2016) 084001, [1601.07459].
- [46] A. Rivas and S. F. Huelga, *Open Quantum Systems*. SpringerBriefs in Physics. Springer, 2012, 10.1007/978-3-642-23354-8.
- [47] G. Lindblad, *On the Generators of Quantum Dynamical Semigroups*, *Commun. Math. Phys.* **48** (1976) 119.
- [48] C. A. Argüelles, J. Salvado and C. N. Weaver, *nuSQuIDS: A toolbox for neutrino propagation*, *Comput. Phys. Commun.* **277** (2022) 108346, [2112.13804].
- [49] M. C. Gonzalez-Garcia, F. Halzen and M. Maltoni, *Physics reach of high-energy and high-statistics icecube atmospheric neutrino data*, *Phys. Rev. D* **71** (2005) 093010, [hep-ph/0502223].
- [50] Y. Farzan, T. Schwetz and A. Y. Smirnov, *Reconciling results of LSND, MiniBooNE and other experiments with soft decoherence*, *JHEP* **07** (2008) 067, [0805.2098].
- [51] J. C. Carrasco, F. N. Díaz and A. M. Gago, *Probing CPT breaking induced by quantum decoherence at DUNE*, *Phys. Rev. D* **99** (2019) 075022, [1811.04982].
- [52] V. De Romeri, C. Giunti, T. Stuttard and C. A. Ternes, *Neutrino oscillation bounds on quantum decoherence*, *JHEP* **09** (2023) 097, [2306.14699].
- [53] E. Lisi, A. Marrone and D. Montanino, *Probing possible decoherence effects in atmospheric neutrino oscillations*, *Phys. Rev. Lett.* **85** (2000) 1166–1169, [hep-ph/0002053].
- [54] G. L. Fogli, E. Lisi, A. Marrone, D. Montanino and A. Palazzo, *Probing non-standard decoherence effects with solar and KamLAND neutrinos*, *Phys. Rev. D* **76** (2007) 033006, [0704.2568].
- [55] B. Kayser, *On the Quantum Mechanics of Neutrino Oscillation*, *Phys. Rev. D* **24** (1981) 110.
- [56] P. H. Frampton and P. Vogel, *MASSIVE NEUTRINOS*, *Phys. Rept.* **82** (1982) 339–388.
- [57] C. Giunti, C. W. Kim and U. W. Lee, *When do neutrinos really oscillate?: Quantum mechanics of neutrino oscillations*, *Phys. Rev. D* **44** (1991) 3635–3640.
- [58] C. Giunti, C. W. Kim, J. A. Lee and U. W. Lee, *On the treatment of neutrino oscillations without resort to weak eigenstates*, *Phys. Rev. D* **48** (1993) 4310–4317, [hep-ph/9305276].
- [59] C. Giunti, C. W. Kim and U. W. Lee, *When do neutrinos cease to oscillate?*, *Phys. Lett. B* **421** (1998) 237–244, [hep-ph/9709494].
- [60] K. Kiers and N. Weiss, *Neutrino oscillations in a model with a source and detector*, *Phys. Rev. D* **57** (1998) 3091–3105, [hep-ph/9710289].
- [61] E. K. Akhmedov and A. Y. Smirnov, *Paradoxes of neutrino oscillations*, *Phys. Atom. Nucl.* **72** (2009) 1363–1381, [0905.1903].
- [62] E. Akhmedov, J. Kopp and M. Lindner, *Decoherence by wave packet separation and collective neutrino oscillations*, 1405.7275.
- [63] J. Kersten and A. Y. Smirnov, *Decoherence and oscillations of supernova neutrinos*, *Eur. Phys. J. C* **76** (2016) 339, [1512.09068].

- [64] D. V. Naumov and V. A. Naumov, *Quantum Field Theory of Neutrino Oscillations*, *Phys. Part. Nucl.* **51** (2020) 1–106.
- [65] I. Esteban, M. C. Gonzalez-Garcia, M. Maltoni, T. Schwetz and A. Zhou, *The fate of hints: updated global analysis of three-flavor neutrino oscillations*, *JHEP* **09** (2020) 178, [2007.14792].
- [66] I. Esteban, M. C. Gonzalez-Garcia, M. Maltoni, T. Schwetz and A. Zhou, “NuFit webpage.” <http://www.nu-fit.org>.
- [67] IceCube Collaboration, *Searching for eV-scale sterile neutrinos with eight years of atmospheric neutrinos at the IceCube Neutrino Telescope*, *Phys. Rev. D* **102** (2020) 052009, [2005.12943].
- [68] A. Cooper-Sarkar, P. Mertsch and S. Sarkar, *The high energy neutrino cross-section in the Standard Model and its uncertainty*, *JHEP* **08** (2011) 042, [1106.3723].
- [69] J. F. Beacom, P. Crotty and E. W. Kolb, *Enhanced Signal of Astrophysical Tau Neutrinos Propagating through Earth*, *Phys. Rev. D* **66** (2002) 021302, [astro-ph/0111482].
- [70] C. A. Argüelles, D. Garg, S. Patel, M. H. Reno and I. Safa, *Tau depolarization at very high energies for neutrino telescopes*, *Phys. Rev. D* **106** (2022) 043008, [2205.05629].
- [71] IceCube Collaboration, “NuFlux: A library for calculating atmospheric neutrino fluxes.” <https://doi.org/10.5281/zenodo.5874708>.
- [72] IceCube Collaboration, *Characteristics of the diffuse astrophysical electron and tau neutrino flux with six years of IceCube high energy cascade data*, *Phys. Rev. Lett.* **125** (2020) 121104, [2001.09520].
- [73] IceCube Collaboration, *Replication Data for: Searching for Decoherence from Quantum Gravity at the IceCube South Pole Neutrino Observatory*, 2024. <https://doi.org/10.7910/DVN/9WGYQN>, 10.7910/DVN/9WGYQN.
- [74] C. A. Argüelles, A. Schneider and T. Yuan, *A binned likelihood for stochastic models*, *JHEP* **06** (2019) 030, [1901.04645].
- [75] IceCube Collaboration, *Evidence for neutrino emission from the nearby active galaxy NGC 1068*, *Science* **378** (Nov., 2022) 538–543.
- [76] IceCube Collaboration, *The design and performance of IceCube DeepCore*, *Astroparticle Physics* **35** (May, 2012) 615–624.